Experimental investigation of the sCO2-HeRo compressor

Hacks, Alexander Johannes; Vojacek, Ales; Dohmen, Hans Josef; Brillert, Dieter

In: 2nd European sCO2 Conference 2018

DOI: https://doi.org/10.17185/duepublico/46088

URN: urn:nbn:de:hbz:464-20180827-132059-0

Link: https://duepublico.uni-duisburg-essen.de:443/servlets/DocumentServlet?id=46088

2nd European supercritical CO2 Conference
August 30-31, 2018, Essen, Germany

2018-sCO2.eu-115

EXPERIMENTAL INVESTIGATION OF THE SCO2-HERO COMPRESSOR

Alexander Hacks
University of Duisburg-Essen
Duisburg, Germany
Email: Alexander.Hacks@uni-due.de

Ales Vojacek
Research Centre Řež
Řež, Czech Republic

Hans Josef Dohmen
University of Duisburg-Essen
Duisburg, Germany

Dieter Brillert
University of Duisburg-Essen
Duisburg, Germany

ABSTRACT

Supercritical CO_2 (sCO2) is widely used in many industrial applications. The utilization of sCO2 power cycles has been gaining attention and first prototypes of the order of few MWe are being built. A European consortium led by University of Duisburg-Essen is investigating a sCO2 heat removal system (sCO2-HeRo) as a back-up cooling system, which efficiently removes residual heat from nuclear fuel without the requirement of external power sources. The sCO2-HeRo system applies a simple sCO2 Brayton cycle. This technical paper presents the first test results of the sCO2 turbomachine (TAC). The paper focuses on the validation of the calculated performance maps of the centrifugal compressor. The tests were performed in the newly built sCO2 experimental loop, which was constructed within the SUSEN (Sustainable Energy) project at Research Centre Řež (CVR).

INTRODUCTION

Raising nuclear reactor safety to a higher level, the sCO2 heat removal system (sCO2-HeRo) is developed within a EU funded project. The objective of this project is to build a small-size demonstrator sCO2 cycle and install it at the PWR glass model at the Gesellschaft für Simulatorschulung mbH (GfS) in Essen, Germany. The glass model allows to simulate different accident scenarios. Thus, the operation of the downscaled unit will demonstrate the maturity of the sCO2-HeRo cycle. The self-propellant, self-sustaining sCO2-HeRo simple Brayton cycle includes a compressor, heat exchanger (steam to sCO2), turbine and sink heat exchanger, whereby the compressor and turbine impellers are mounted onto one shaft with a generator in between [1]. Each of the components is pre-tested before final assembling into the sCO2-HeRo cycle at GfS. The turbomachine pre-tests were conducted at CVR to validate the calculated performance maps and gain knowledge on the machine behaviour.

DESCRIPTION OF TURBOMACHINE-SET FOR THE GLASS MODEL

The tested TAC has an integrated design and consists of three major components turbine, alternator and compressor. The cross section of the TAC and pictures of the impellers are presented in Figure 1. Figure 1 also includes the flow directions of the sCO2 through the machine and gives an impression on the impeller dimensions. As shown in Figure 1 the compressor is on the left and the turbine on the right, while the alternator is in the middle. The bearings are realized by angular hybrid ball bearings in between the impellers and the generator respectively. The thrust bearing is on the side of the compressor. Both compressor and turbine consist of one stage and have shrouded impellers with 2D-radial blading. This allows for labyrinth seals to be applied, which reduce the leakage losses. These losses have a significant influence on the components efficiency due to the small mass flow within the cycle. Table 1 contains the cycle mass flow and further thermodynamic conditions. The mass flow is limited by the heating power of the glass model, while the maximum temperature at the turbine inlet refers to the operating conditions of a nuclear power plant for emergency cooling. The compressor inlet lies close to the critical point reducing the compression work. For further information on the test cycle and cycle parameters please refer to Benra et al. [1]. Due to the given thermodynamic parameters and maximum mass flow the type and dimension of the compressor and turbine (shown in Figure 1) are chosen. The nominal rotational speed of the shaft is 50,000 rpm with an electrical power of the motor of 7 kW. For more information on the TAC design and the design procedure please refer to Hacks et al. [3].

DOI: 10.17185/duepublico/46088

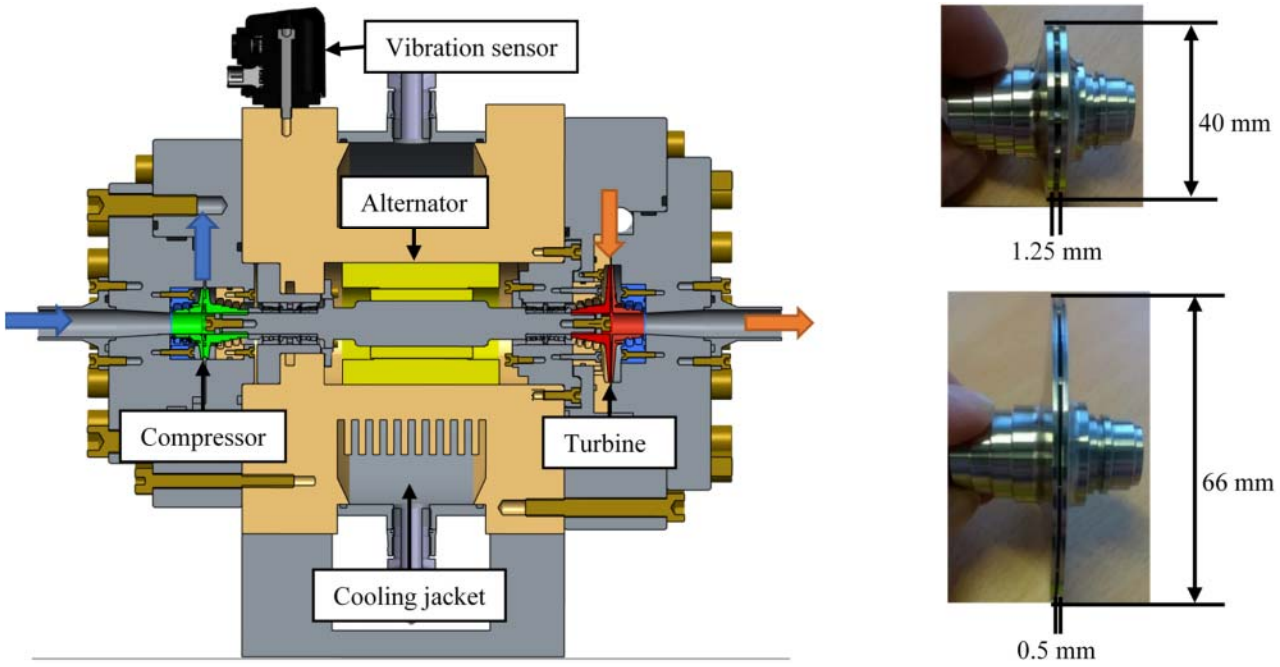

Figure 1: Cross section and impellers of the TAC with flow directions and dimensions

Table 1: Nominal conditions at cycle interfaces

Component	Parameter	Value
Compressor inlet	Pressure	78.3 bar
	Temperature	33 °C
	Mass flow	0.65 kg/s
Compressor outlet	Pressure	117.5 bar
	Mass flow	0.65 kg/s
Turbine inlet	Pressure	117.5 bar
	Temperature	200 °C
	Mass flow	0.65 kg/s
Turbine outlet	Pressure	78.3 bar
Leakage	Pressure	65 bar

TEST FACILITY

The turbomachine performance test took place at Research Centre Rez, using the SUSEN sCO2 experimental loop. This unique facility enables to study key aspects of the cycle (turbomachines, heat transfer, erosion, corrosion etc.) with a wide range of design parameters [7]:

- Temperature: up to 550°C
- Pressure: up to 300 bar
- Mass flow rate: up to 0.35 kg/s (limited by the circulation piston pump) As the sCO2-HeRo compressor is used the mass flow is raised to 0.65 kg/s

Figure 2 shows the piping and instrument diagram (PID) of the loop. The part of the primary circuit used for the TAC measurement is marked by the red connection lines. The main components are:

- The turbomachine (TAC), which consist of the turbine, alternator and compressor [3].
- The circulation piston pump returns the leakage from the TAC back to the cycle and is used for circulation during cycle warm-up.
- The high and low temperature regenerative heat exchanger (HTR HX/LTR HX) reduce the heating and cooling power.
- The 4 electric heaters (H1/1, H1/2, H2, H3) have in total a maximum power of 110 kW.
- The water coolers CH1 and the leakage cooler.

The heat exchangers HTR HX and LTR HX are designed as counter-flow shell and tube-type from stainless steel. Each heater concludes of 12 heating elements made from specially designed electric heating rods, which are encapsulated in austenitic steel (for H1/1, H1/2, H3) or Inconel (for H2) pressure boundary. The pressure in the system is controlled either by the electric heaters, i.e. by the temperature in the circuit, or by inventory control strategy. This concludes of the filling compressor and the release valves (to the outside atmosphere), by which it is possible to control the amount of CO2 in the loop and thus the pressure. To protect the loop several pressure relief valves are installed at different positions. Excess pressure is expected e.g. at the outlet of the heating parts as well as the compressor and the pumps.

DOI: 10.17185/duepublico/46088

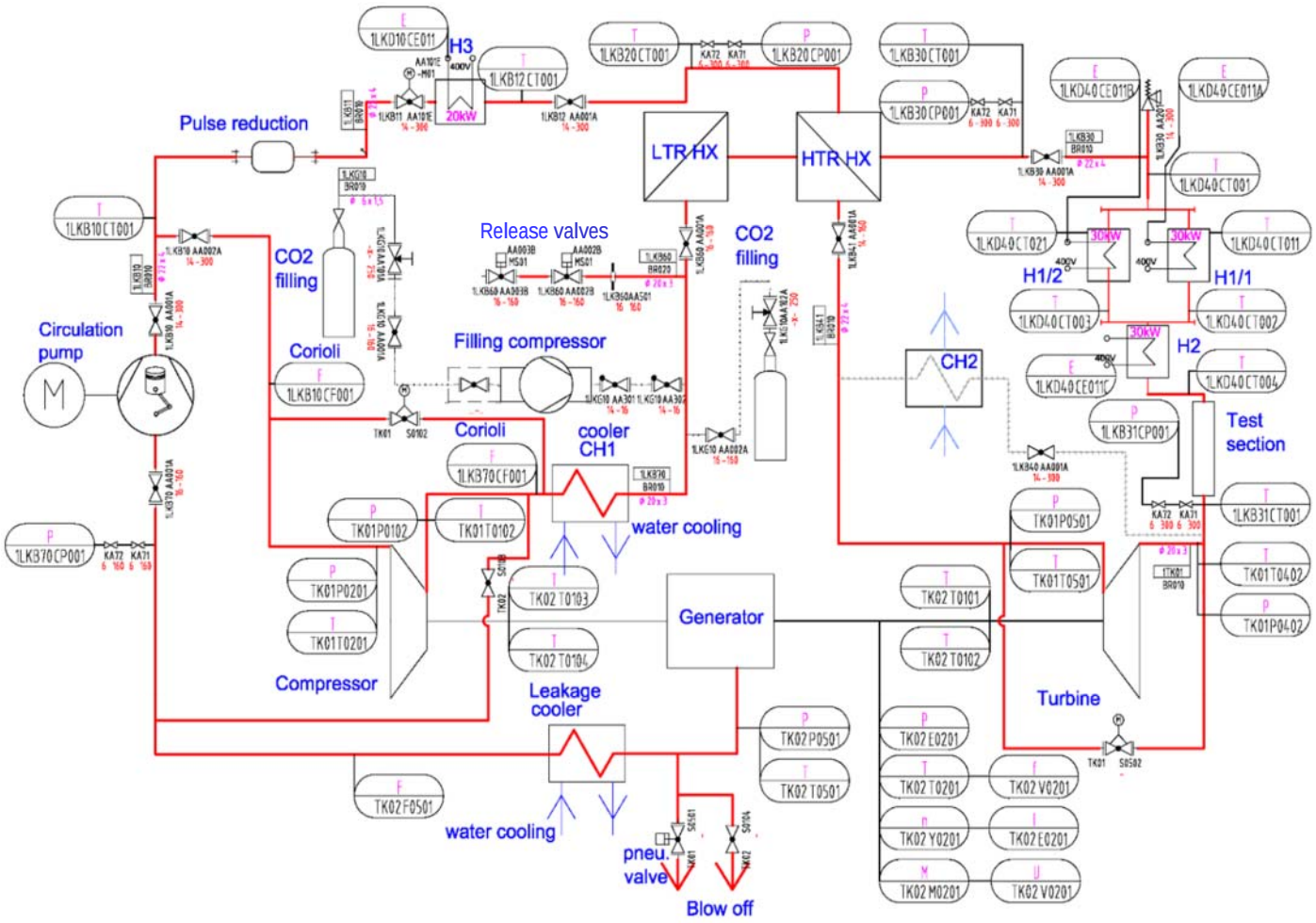

Figure 2: PID of the sCO2 loop with TAC at CVR

MEASUREMENT DEVICES AND ERRORS

Measuring the momentum or power of the motor to determine the compressor power is not possible in the machine configuration shown in Figure 1, because the turbine is mounted to the same shaft and windage losses have a significant influence on the required motor power. Figure 2 shows the piping and installation diagram (PID diagram) of the modified sCO_2 loop with the main components together with all installed measurement devices. These are mass flow meters, Pt-100 sensors, thermocouples, pressure sensors, vibration sensors etc. The nomenclature of the measurement devices respects the KKS identification system for power plants. The uncertainties provided by the measurement devices, transducers, input cards and the control system are summarized in Table 2. The errors correspond to calibration certificates and the manufacturer's instructions. The error propagations of the measuring errors are described in Annex A.

DOI: 10.17185/duepublico/46088

Table 2: Installed measurement devices and errors (in percent of range)

Description	Variable	Range	Unit	Device error	Transducer error	Input card error	Control system error	Total error
Mass flow rate 1LKB70CF001, 1LKB10CF001 Rheonik (RHM12)	$\dot{m}_{comp\_in}$ $\dot{m}_{comp\_out}$	0 – 0.7	kg/s	0.15 % from 1.66 kg/s	Rawet – PX310S 0.1 %	Siemens SM 331 0.4 %	ABB freelance 0.1 %	+/- 0.007 kg/s
Compressor inlet temperature, JSP (Pt 100)	T_{comp_in}	15 – 45	°C	0.15 %	Rawet – PX310S 0.1 %	Siemens SM 331 0.4 %	ABB freelance 0.1 %	+/- 0.26 K
Compressor outlet temperature, JSP (Pt 100)	T_{comp_out}	15 – 60	°C	0.15 %	Rawet – PX310S 0.1 %	Siemens SM 331 0.4 %	ABB freelance 0.1 %	+/- 0.35 K
Turbine inlet/outlet and leakage temperature, TC (type K) , Omega	T_{turb_in} T_{turb_out} $T_{leakage}$	0 – 600	°C	0.275 %	Rawet – PX310S 0.1 %	Siemens SM 331 0.4 %	ABB freelance 0.1 %	+/- 5.1 K
Compressor pressure inlet/outlet, Turbine pressure outlet, GE (UNIK 5000)	p_{comp_in} p_{comp_out} p_{turb_out}	0 – 150	bar	0.15 %	Rawet – PX310S 0.1 %	Siemens SM 331 0.4 %	ABB freelance 0.1 %	+/- 1.1 bar
Turbine pressure inlet, leakage pressure, GE (UNIK 5000)	p_{turb_in} $p_{leakage}$	0 – 300	bar	0.15 %	Rawet – PX310S 0.1 %	Siemens SM 331 0.4 %	ABB freelance 0.1 %	+/- 2.3 bar

PERFORMANCE TESTS

The main objective of the performance tests is the validation of the calculated performance maps of both compressor and turbine. The performance maps are introduced into the German nuclear code ATHLET to predict the cycle behaviour and thus introduce the HeRo safety system into nuclear power plants. In general, performance maps show the characteristic behaviour of compressors and turbines. Usually the pressure ratio, specific work or efficiency is plotted against the flow rate or flow coefficient for different rotational speeds. Figure 3 shows an example of such a performance map showing the pressure ratio over the flow coefficient for different speeds. The pressure ratio and efficiency are combined into one diagram. In general compressor performance maps also include the surge line (b) and choke line (c). Figure 3 additionally includes the blow-off (d) and stability line (a). Point A represents the design point. The stability and surge line represent the lower border of flow rate at a given speed for which the flow through the compressor gets unstable due to flow separation at the suction side of the blades. The choke line on the other hand represents the upper border at which the flow through the compressor gets choked. The blow-off line indicates the flow rate at which measures, such as blowing-off a part of the gas flow, should be taken to prevent unstable operation and surge. To measure the performance map, the inlet and outlet conditions of the compressor or turbine need to be measured as well as the rotational speed. The TAC shall start-up by itself, if a station blackout occurs. Further, the decay heat reduces during operation. It is therefore necessary to know the behaviour of the machine at off-design conditions. The performance maps are thus measured for different inlet conditions.

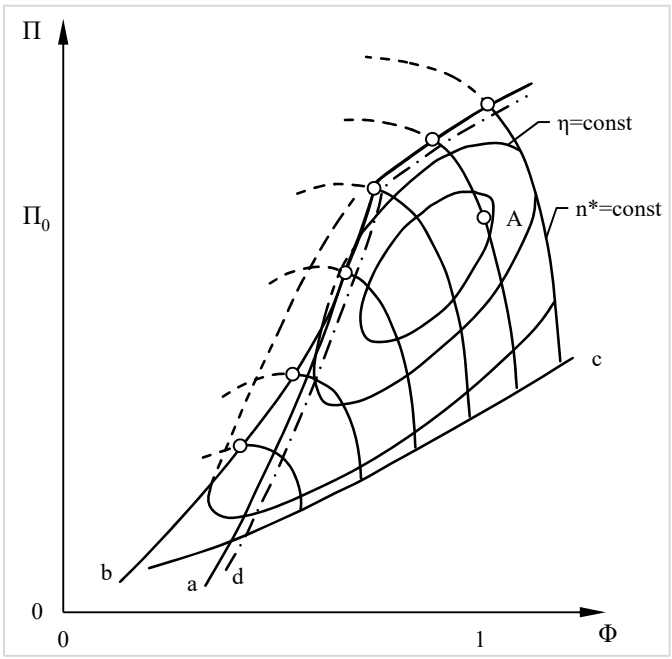

Figure 3: Compressor performance map according to Traupel (Abb. 13.2.1. Page 104 [6])

DOI: 10.17185/duepublico/46088

MEASUREMENT PARAMETERS

The performance test shall give insight in the machine performance within the expected range of operation and the general machine and cycle behaviour. As the dependency of fluid properties of sCO2 on pressure and temperature is especially large close to the critical point the performance map of the compressor regarding different inlet conditions is of great importance. The performance testing is separated in several test sequences. Each covers a certain objective leading to a certain range of parameters. Measurements are taken at stationary conditions meaning without fluctuations in mass flow, pressure and temperature and then compared to the regarding CFD calculations. The approach to the CFD calculations is described by Hacks et al. [3] and Schuster et al. [5]. The test sequences and the regarding parameters are summarized in Table 3. The main objectives and the approaches are as follows.

1) **Objective**: Find a strategy for starting the cycle including the TAC and bringing it to nominal conditions.
   Approach: Fill the loop with CO_2 from the bottle. Then bring the loop to nominal conditions by heating up the CO_2 and thus also increasing its pressure (because the loop is a closed volume) to reach supercritical conditions and start the TAC using the generator as motor.
2) **Objective**: Measure the compressor performance map.
   Approach: Bring the compressor inlet conditions to the desired conditions using knowledge from test sequence 1. Vary the conditions at the compressor inlet. The turbine conditions are also monitored but turbine inlet conditions do not need to be stationary. At speeds higher than 30000 rpm the turbine is used to provide auxiliary power to turn the compressor
3) **Objective**: Measure the turbine performance map.
   Approach: Bring the turbine inlet conditions to the desired conditions using knowledge from test sequence 1 and 2. Vary the conditions at the turbine inlet. The turbine mass flow and inlet pressure are dependent on the compressor performance. The mass flow through the turbine is set by splitting up the mass flow through the compressor and let a fraction bypass the turbine.
4) **Objective**: Check bearing operation in sCO2.
   Approach: In the previous tests the central housing is held at constant subcritical pressure of 65 bar. Now pressure is varied by changing the mass flow through the leakage pump.

Table 3: Test sequences and parameters

Test sequence	Test parameters						
	Mass flow $\dot{m}_{sCO2}$ (kg/s)	**Compressor p_{in} (bar)**	**Compressor T_{in} (°C)**	**Turbine p_{in} (bar)**	**Turbine T_{in} (°C)**	**Leakage p_{out} (bar)**	**Speed n (rpm)**
1 – Start-up test	resulting	resulting	resulting	resulting	resulting	65 (max.)	0-50,000
2 – Compressor test	0.3 - 0.7	77.3 - 79.3	31.5 - 34.5	resulting	resulting	65 (max.)	10,000-50,000
3 – Turbine test	0.3 - 0.7	78.3	33	resulting	150 - 200	65 (max.)	10,000-50,000
4 – Central housing test	resulting	78.3	33	resulting	150	55 - 117.5	10,000

EXPERIMENTAL RESULTS AND DISCUSSION

The previously described test plan was taken as basis for the actual testing. Test sequence 1 regarding the start-up and test sequence 4 regarding the pressure in the central housing showed limitations of testing in the SUSEN loop at CVR. For start-up testing the cycle is filled from CO_2 bottles to a pressure of up to 60 bar. The circulation pump is used to circulate the CO2 in the cycle and through the heaters. The turbomachine is bypassed. During circulation the CO_2 is heated up until the cycle reaches supercritical conditions. During this procedure the valves to the turbomachine are opened as soon as gaseous inlet conditions are reached at all turbomachine inlets. Thus, also the turbomachine is preheated. To set the desired compressor inlet conditions CO_2 is either added or released by the filling compressor or release valves respectively. Then the turbomachine is started. During first start-up, it was noticed that the overall pressure drop in the cycle is too big for the turbine to be tested in closed loop configuration together with the compressor. The reason for the high pressure losses is that the test facility is originally designed for a lower flow rate and for high temperatures, which require recuperators to reduce the heating and cooling power. Therefore, the compressor is tested in bypass configuration employing valve TK02 S0102 (see Figure 2) as a throttle. The turbine tests are dismissed and will be done at the GfS. Pressure rise in the central housing and thus sCO2 at the bearings showed that the grease lubricated bearings cannot operate in sCO2 and that it must be ensured that the CO_2 in the central housing is always gaseous. Thus, the pressure in the central housing is limited to

DOI: 10.17185/duepublico/46088

68 bar by a pressure relieve valve. To ensure delivery to GfS within the target time frame and because of the very limited auxiliary power of the turbine caused by the low turbine mass flow (leakage only), performance map testing was only carried out for a rotational speed of up to 30,000 rpm.

Affinity laws

It is found that affinity laws according to Bohl and Elmendorf [2], as stated in Table 4, are sufficiently accurate to predict the performance for other operation conditions such as other compressor inlet conditions and other rotational speeds. Figure 4 indicates this for 30,000 rpm, showing the measured pressure ratio at 30,000 rpm versus the pressure ratio for 30,000 rpm calculated by the affinity laws from the pressure ratio measured for 20,000 rpm and 25,000 rpm respectively. The maximum difference between the pressure ratio predicted by the affinity laws and the actual measured pressure ratio is less than 0.003 or an error of 2 % regarding the measured pressure increase across the compressor. As a conclusion the performance data for one rotational speed is measured for three different inlet conditions. Measurements are taken once for the design conditions with the nominal density at the compressor inlet and once for higher and lower density respectively. The desired performance data for other inlet conditions is calculated by the affinity laws. This allows implementation into the nuclear code ATHLET by implementing the measured data and interpolating this data using the affinity laws.

Table 4: Parameters for affinity laws [2]

Speed ratio	$k_n = \frac{n_I}{n_{II}}$	(1)
Size ratio	$k_d = \frac{d_I}{d_{II}}$	(2)
Density ratio	$k_\rho = \frac{\rho_I}{\rho_{II}}$	(3)
Mass flow	$\frac{\dot{m}_I}{\dot{m}_{II}} = k_d^3 * k_n * k_\rho$	(4)
Pressure difference	$\frac{\Delta p_I}{\Delta p_{II}} = k_d^2 * k_n^2 * k_\rho$	(5)
Efficiency[1]	$\frac{\eta_I}{\eta_{II}} = 1 \ or$ $Pfleiderer: \frac{1-\eta_{II}}{1-\eta_I} = \left(\frac{Re_I}{Re_{II}}\right)^{0.1}$ $Re = \frac{d^2 * \omega}{\nu}$	(6)
Power	$\frac{P_I}{P_{II}} = k_d^5 * k_n^3 * k_\rho$	(7)

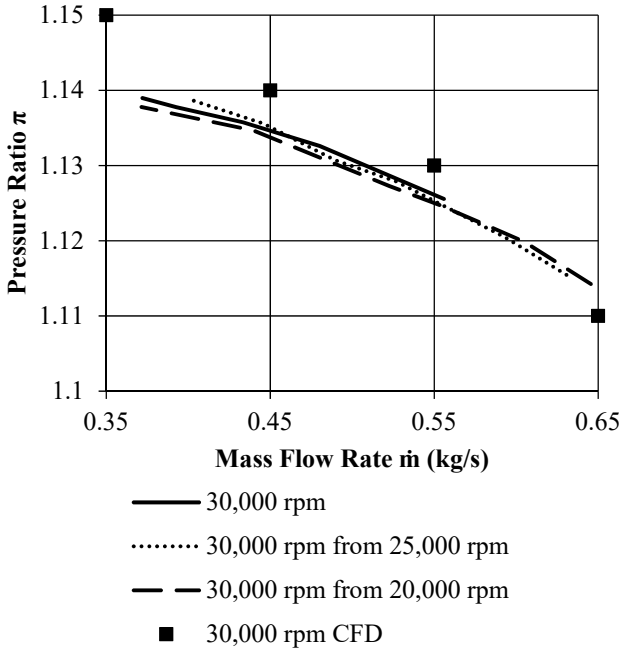

Figure 4: Affinity law applied for 30000 rpm

Compressor performance map

Figure 5 shows the pressure ratio performance map of the compressor in terms of pressure ratio versus compressor inlet mass flow for three different inlet conditions indicated by different symbols. The inlet conditions refer to the minimum and maximum as well as the nominal inlet density into the compressor. This means inlet conditions with maximum inlet temperature and minimum pressure, minimum inlet temperature and maximum pressure and nominal conditions according to Table 3. The error bars are calculated according to the formulas in Annex A. They are similar for different inlet conditions and thus only shown for the nominal inlet conditions to improve readability of the diagram. The surge line indicates the position at which the calculated performance lines have their maximum. The pressure ratio thus raises from the working point towards the predicted surge line in accordance with API Standard 617 (Lüdtke [4]). The calculated performance lines and the surge line are for nominal inlet conditions only. Figure 5 presents that the measured pressure ratios for nominal inlet conditions correspond closely to the pressure ratios calculated using CFD. They tend to underestimate the CFD results only for higher speeds. Still the values calculated with CFD lie within the uncertainty range indicated by the error bars. These get especially large due to error propagation, if affinity laws are applied. In general affinity laws consider constant efficiency. Increase in efficiency can be expected with increasing speed according to the formula of Pfleiderer [2]. Anyhow, this increase is not considered in the

[1] Formula of Pfleiderer is taken from the book of Bohl and Elmendorf [2]

DOI: 10.17185/duepublico/46088

calculation of the pressure ratio. Therefore, the pressure ratios for 40,000 rpm and 50,000 rpm are conservative values.

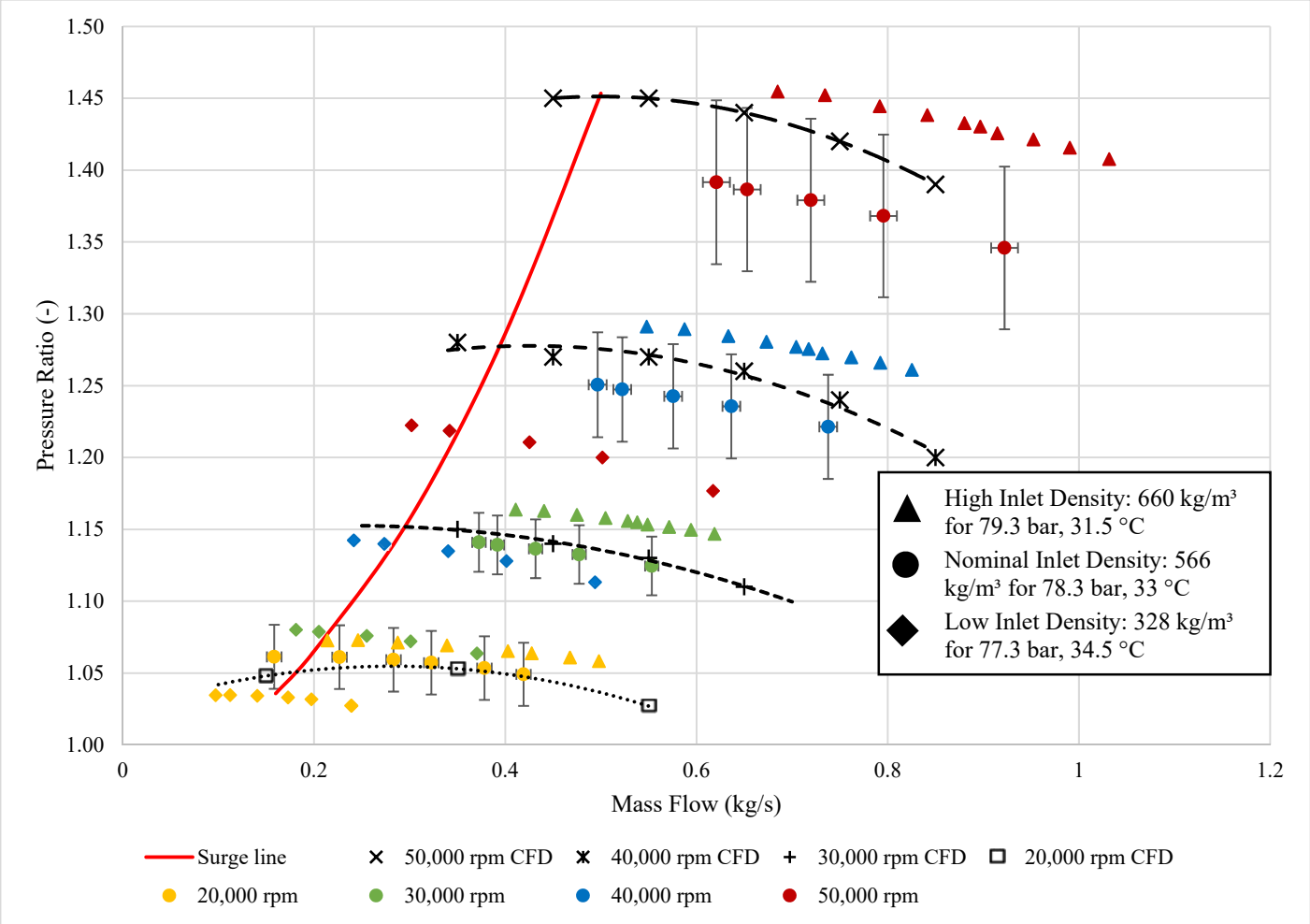

Figure 5: Compressor performance map – Pressure ratio

It is found that the pressure ratio raises with the inlet density and vice versa. The differences in the measured pressure ratio are large with respect to changing inlet conditions. But on the other hand, this shows that changing the inlet conditions in a way that the inlet density increases also raises the pressure ratio. The previously mentioned difference between calculated and measured pressure ratio at high rotational speeds can therefore be balanced by reducing the temperature at the compressor inlet. The isentropic efficiency and the power of the compressor calculated from the measured pressures and temperatures show huge uncertainties. They are caused by the small enthalpy difference between compressor inlet and outlet combined with the strong dependency of the enthalpy on the inlet conditions. As the uncertainties are as big as the calculated value itself neither the isentropic efficiency nor the calculated power is presented here. The measurements at GfS will be used to get further insight into the compressor power and efficiency. Systematical measurement errors must be minimized and all measurement devices must be calibrated in assembled conditions.

CONCLUSIONS

The turbomachine tests at CVR gave insight in the cycle behaviour and showed a possible start-up procedure of the sCO2 cycle, which can also be applied for the HeRo cycle at GfS. It is found that grease lubricated ball bearings need to be operated in gaseous CO_2 to ensure operability.

The compressor performance measurements of the pressure ratio matched well with the CFD calculations. Strategies to increase pressure ratio were found. To increase the pressure ratio the temperature at the compressor inlet can be decreased and thus also the density increased. It is therefore possible to adjust the compressor pressure ratio, if it is required, for further testing at GfS.

DOI: 10.17185/duepublico/46088

Calculated efficiency and power are not presented as the uncertainties of the measurements are large. For calculating these parameters accurately, the pressure and temperature measurements need to be very accurate. Calibration of the measurement devices connected to the control system is essential.

NOMENCLATURE

Measurement in KKS code	Description
TK01T0102	Inlet temperature to the compressor
TK01T0201	Outlet temperature of the compressor
TK01P0102	Inlet pressure to the compressor
TK01P0201	Outlet pressure of the compressor
TK01T0402	Inlet temperature to the turbine
TK01T0501	Outlet temperature of the turbine
TK01P0402	Inlet pressure to the turbine
TK01P0501	Outlet pressure of the turbine
TK02T0501	Leakage temperature
TK02P0501	Leakage pressure
1LKB70CF001	Mass flow rate inlet to the compressor
1LKB10CF001	Mass flow rate outlet from the compressor to the loop without the recirculating part which bypass the loop
TK02F0501	Leakage mass flow rate

Abbreviations	Description
CH1	Water cooler
CH2	Oil cooler
CVR	Research Centre Řež
GfS	Gesellschaft für Simulatorschulung mbH in Essen, Germany
H1/1, H1/2, H2 and H3	Electric heaters
HTR	High temperature regenerative heat exchanger
LTR	Low temperature regenerative heat exchanger
PID	Piping and installation diagram
sCO2	Supercritical carbon dioxide
sCO2-HeRo	Supercritical carbon dioxide heat removal system
SUSEN	Sustainable Energy project
TAC	Turbomachine

Variable	Unit	Description
cp	kJ/(kg*K)	Isobaric heat capacity
d	mm	Diameter
h	kJ/kg	Enthalpy
k_n	-	Speed ratio
k_d	-	Size ratio
k_ρ	-	Density ratio
$\dot{m}$	kg/s	Mass flow rate
n	1/min	Rotational speed
p	bar	Pressure
Δp	bar	Pressure drop
P	kW	Power
Q	m^3/s	Volume flow
Re	-	Reynolds number
T	K	Temperature
η	%	Efficiency (isentropic)
ν	m^2/s	Kinematic viscosity
π, Π	-	Pressure ratio
ρ	kg/m^3	Density
σ	n.a.	Error propagation
Φ	-	Flow coefficient
ω	1/s	Angular velocity

Subscripts	Description
comp	Compressor
in	Inlet
is	Isentropic
leakage	Leakage
out	Outlet
turb	Turbine
I	Target parameter for calculation by affinity law
II	Base parameter for calculation by affinity law

ACKNOWLEDGEMENTS

This project has received funding from the European research and training programme 2014 – 2018 under grant agreement No 662116.

DOI: 10.17185/duepublico/46088

REFERENCES

[1] Benra, F.-K., Brillert, D., Frybort, O., Hajek, P., Rohde, M., Schuster, S., Seewald, M. & Starflinger, J. (2016). A supercritical CO2 low temperature Brayton-cycle for residual heat removal. *The 5th International Symposium - Supercritical CO2 Power Cycles*, San Antonio, Texas, USA

[2] Bohl, W. & Elmendorf, W. (2013). *Strömungsmaschinen 1. Aufbau und Wirkungsweise* (Vol. 11). Würzburg: Vogel

[3] Hacks, A. J., Schuster, S., Dohmen H. J., Benra F.-K. & Brillert D. (2018). Turbomachine Design for Supercritical Carbon Dioxide within the sCO2-HeRo.eu Project. *ASME Turbo Expo*, Oslo, Norway

[4] Lüdtke, K. H. (2004) *Process Centrifugal Compressors – Basics, Function, Operation, Design, Application*. Springer Science and Business Media

[5] Schuster, S., Benra, F.-K., Brillert, D. (2016) Small scale sCO2 compressor impeller design considering real fluid conditions. *The 5th International Symposium - Supercritical CO2 Power Cycles*, San Antonio, Texas, USA

[6] Traupel, W. (2001) *Thermische Turbomaschinen 2* (Vol 4). Springer-Verlag

[7] Vojacek, A., Hacks, A. J., Melichar, T., Frybort, O. & Hajek, P. (2018). "First Operational Experience from the Supercritical CO2 Experimental Loop. *2nd European supercritical CO2 Conference*, Essen, Germany

DOI: 10.17185/duepublico/46088

ANNEX A

ERROR PROPAGATION

The following shows the calculation off the error propagation of pressure ratio and mass flow for direct calculation from the measurements and for application of the affinity laws.

Pressure difference: $$\sigma_{\Delta p} = \sqrt{\left(\sigma_{p_{in}}\right)^2 + \left(\sigma_{p_{out}}\right)^2} \tag{8}$$

Pressure ratio: $$\sigma_{\pi} = \sqrt{\left(-\frac{p_{out}}{p_{in}^2} * \sigma_{p_{in}}\right)^2 + \left(\frac{1}{p_1} * \sigma_{p_{out}}\right)^2} \tag{9}$$

For the calculation of the error propagation due to the use of the affinity laws the following assumptions are taken as simplification:

$$\sigma_{k_d} = \sigma_{k_n} = \sigma_{k_\rho} = 0 \tag{10}$$

Further the machine is always the same, which implies:

$$k_d = 1 \tag{11}$$

Mass flow by affinity law: $$\sigma_{\dot{m}_I} = k_n * k_\rho * \sigma_{\dot{m}_{II}} \tag{12}$$

Pressure ratio by affinity law: $$\sigma_{\Delta p_I} = \sqrt{\left(\frac{1}{p_{in}} * k_n^2 * k_\rho * \sigma_{\Delta p_{II}}\right)^2 + \left(-\frac{\Delta p_I}{p_{in}^2} * \sigma_{p_{in}}\right)^2} \tag{13}$$

DOI: 10.17185/duepublico/46088